Asociación Argentina
de Mecánica Computacional

Mecánica Computacional Vol XXIX, págs. 2549-2561 (artículo completo)
Eduardo Dvorkin, Marcela Goldschmit, Mario Storti (Eds.)
Buenos Aires, Argentina, 15-18 Noviembre 2010

COARSE-MESH DIFFUSION SYNTHETIC ACCELERATION OF THE SCATTERING SOURCE ITERATIVE SCHEME FOR ONE-SPEED DISCRETE ORDINATES NEUTRON TRANSPORT CALCULATIONS IN SLAB GEOMETRY

Frederico P. Santos[a],Vinicius S. Xavier[b]; Hermes Alves Filho[a], Ricardo C. Barros[a]

[a]*Programa de Pós-graduação em Modelagem Computacional,* [b]*Instituto Politécnico, Universidade do Estado do Rio de Janeiro, Rua Alberto Rangel s/n 28630-050 Nova Friburgo, RJ, Brasil, fpsantos@iprj.uerj.br, vinicius__xavier@hotmail.com, halves@iprj.uerj.br, rcbarros@pq.cnpq.br*

Keywords: neutral particle transport, discrete ordinates**,** source iteration, diffusion synthetic acceleration

Abstract. The scattering source iterative (SI) scheme is traditionally applied to converge fine-mesh numerical solutions to fixed-source one-speed discrete ordinates (S_N) neutron transport problems. The SI scheme is very simple to implement under a computational viewpoint. However, the SI scheme may show very slow convergence rate, mainly for diffusive slabs (low absorption) with several mean free paths in extent. In this work we describe an acceleration technique based on an improved initial guess for the scattering source distribution within the slab. In other words, we use as initial guess for the fine-mesh scattering source, the coarse-mesh solution of the neutron diffusion equation with special boundary conditions to account for the classical S_N prescribed boundary conditions, including vacuum boundary conditions. Therefore, we first implement a spectral nodal method that generates coarse-mesh diffusion solution that is completely free from spatial truncation errors, then we reconstruct this coarse-mesh solution within each spatial cell of the discretization grid, to further yield the initial guess for the fine-mesh scattering source to begin the S_N transport sweep (forward and backward) across the spatial grid. We consider a number of numerical experiments to illustrate the efficiency of the offered acceleration technique.

1 INTRODUCTION

The transport phenomena in which the rarefied neutral particles, such as neutrons or photons, interact directly with the dense atoms of the background material, but not with each other, are mathematically described by an integro-differential equation, known as linearized Boltzmann equation [1]. Deterministic computational modeling of particle transport classically leads to the discretization of the linearized Boltzmann equation into a system of linear algebraic equations. Since this system has typically large size, iterative schemes are usually chosen, instead of direct solution methods. To introduce the mathematical basis, let us consider a steady-state, one-speed, isotropically-scattering, fixed-source neutron transport problem in slab geometry

$$\mu\frac{\partial}{\partial x}\psi(x,\mu)+\sigma_T(x)\psi(x,\mu)=\frac{1}{2}\sigma_S(x)\int_{-1}^{1}\psi(x,\mu')d\mu'+Q(x), \qquad 0\le x\le X, \qquad -1\le\mu\le 1 \quad , \tag{1}$$

subjet to the boundary conditions

$$\psi(0,\mu)=f(\mu), \qquad 0<\mu\le 1 \tag{2}$$

and

$$\psi(X,\mu)=g(\mu), \qquad -1\le\mu<0. \tag{3}$$

This notation is standard [1], i.e., x = position; $\mu=\cos\theta$; θ = angle of flight relative to positive x-axis; $\sigma_T(x)$ and $\sigma_S(x)$ are respectively total and scattering macroscopic cross sections; $Q(x)$ is the fixed isotropic source; $f(\mu)$ and $g(\mu)$ are respectively prescribed incident angular flux on the left and right boundaries of problem (1)-(3).

At this point, to simplify notations, we write Eq.(1) in the form

$$L\psi=S\psi+Q(x), \tag{4}$$

where we have defined the migration-plus-collision operator

$$L=\mu\frac{\partial}{\partial x}+\sigma_T(x) \tag{5}$$

and the scattering operator

$$S=\frac{1}{2}\sigma_S(x)\int_{-1}^{1}(\cdot)d\mu' \ . \tag{6}$$

The most basic transport iteration scheme is source iteration (SI), which is defined as

$$L\psi^{(\ell+1)}=S\psi^{(\ell)}+Q(x), \qquad \ell\ge 0, \tag{7}$$

where $\psi^{(0)}$ is initialized by the user [2]. The SI algorithm has the following steps: (i)

one introduces an estimate for the scalar flux

$$\phi(x) = \int_{-1}^{1} \psi(x, \mu') d\mu' \tag{8}$$

in the right-hand side of Eq.(1); (ii) using this estimate, Eq.(1)-(3) are solved for ψ; (iii) this estimate for ψ so obtained is introduced into Eq.(8) to obtain the new estimate for ϕ. This iterative scheme is repeated until a preassigned convergence criterion is satisfied. At this point we remark that if the initial guess for the scalar flux $\phi^{(0)} = 0$ and the ℓ-th estimate of the angular flux is defined as $\psi^{(\ell)}$, then for $\ell \geq 1$, we conclude that $\psi^{(\ell)}(x, \mu)$ is the angular flux due to particles that have scattered at most $\ell - 1$ times. Therefore, for slabs composed of optically thick (low leakage) and scattering-dominated spatial regions, particles in these spatial regions typically undergo many collisions before they are captured or leak out. For such systems, the SI scheme converges slowly and efficient acceleration strategies are of great interest for computational modeling [2].

It is well know that synthetic acceleration techniques are very efficient. The concept of a synthetic acceleration scheme was introduced by Kopp [3], who used the diffusion equation [4] as the low-order operator to accelerate transport iterations. Reed [5] showed that diffusion synthetic method is rapidly convergent for fine spatial grids, but it diverges for coarser grids. Alcouffe [6] proposed a remedy for the divergence described by Reed, introducing the efficient diffusion synthetic acceleration (DSA), which is rapidly convergent for all spatial mesh thicknesses.

In this paper, we describe an acceleration scheme based on an improved initial guess for the scattering source distribution within the slab. In other words, we use as initial guess for the fine-mesh scattering source, the coarse-mesh solution of the neutron diffusion equation with special boundary conditions to account for the classical prescribed boundary conditions in the discrete ordinates (S_N) formulation of neutron transport equation [1]. Therefore, we first implement a spectral nodal method that generates coarse-mesh diffusion solution that is completely free from spatial truncation errors, then we reconstruct this coarse-mesh solution within each spatial cell of the discretization grid, to further yield the initial guess for the fine-mesh scattering source in the first S_N transport sweep ($\mu_m > 0$ and $\mu_m < 0$, $m = 1:N$) across the spatial grid.

Now we give an outline of the remainder of this paper. In the next section we describe the S_N formulation of neutron transport equation in slab geometry and a classical fine-mesh method for numerically solving the S_N equations. In section 3, we present the neutron diffusion equation in slab geometry, the approximate boundary conditions to account for the prescribed boundary conditions traditionally used in S_N problems, the diffusion spectral nodal method and the within-node reconstruction scheme. In section 4 we consider a number of numerical experiments to illustrate the

efficiency of the offered coarse-mesh diffusion synthetic acceleration scheme and a brief discussion is given in section 5.

2 THE DISCRETE ORDINATES MODEL

2.1 The S_N equation

The discrete ordinates (S_N) approximation to the transport equation (1) discretizes the angular variable μ into N discrete values and, as a result, the integral source term in Eq. (1) is approximated by a quadrature formula. In slab geometry, Gauss-Legendre angular quadrature sets [1] are traditionally used, but other angular quadratures can also be considered for the approximation [7]. Therefore, the steady-state, one-speed, isotropically-scattering, fixed source S_N equations in slab geometry appear as

$$\mu_m \frac{d}{dx}\psi_m(x) + \sigma_T(x)\psi_m(x) = \frac{1}{2}\sigma_S(x)\sum_{n=1}^{N}\psi_n(x)\omega_n + Q(x), \qquad \begin{matrix} 0 \le x \le X, & m = 1:N, \end{matrix} \tag{9}$$

with the boundary conditions

$$\psi_m(0) = f_m, \qquad \mu_m > 0 \tag{10}$$

and

$$\psi_m(X) = g_m, \qquad \mu_m < 0. \tag{11}$$

Here, in accordance with Eqs. (1)-(3), we have defined $\psi_m(x) = \psi(x, \mu_m)$, $f_m = f(\mu_m)$, $g_m = g(\mu_m)$ and ω_n as the quadrature weights, $n = 1:N$.

2.2 The fine-mesh linear diamond method

Let us consider a discretization spatial grid set up on a given slab of thickness X as illustrated in Figure 1. On this spatial grid, each discretization cell Γ_j, $j = 1:J$, has thickness h_j, constant cross sections σ_{Tj} and σ_{Sj} and constant source Q_j.

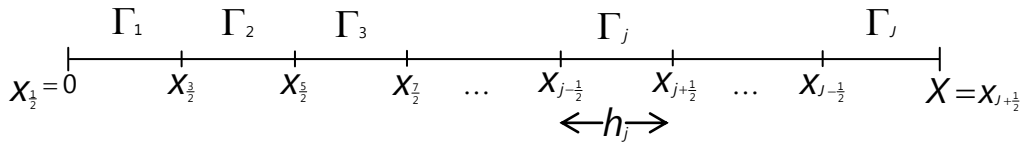

Figure 1: Spatial Discretization Grid

Now we apply the operator

$$\frac{1}{h_j}\int_{x_{j-\frac{1}{2}}}^{x_{j+\frac{1}{2}}}(\cdot)dx$$

to Eq.(9). The result is the standard spatially discretized S_N balance equations

$$\frac{\mu_m}{h_j}\left(\psi_{m,j+\frac{1}{2}}-\psi_{m,j-\frac{1}{2}}\right)+\sigma_{Tj}\overline{\psi}_{m,j}=\frac{1}{2}\sigma_{Sj}\sum_{n=1}^{N}\overline{\psi}_{n,j}\omega_n+Q_j,$$
$$m=1:N, \qquad j=1:J. \tag{12}$$

Equations (12) yield $N\times J$ equations that together with the boundary and the continuity conditions lead to a system of $2NJ$ algebraic equations in $3NJ$ unknowns; therefore we need NJ auxiliary equations to guarantee the uniqueness of the solution. The linear diamond auxiliary equations [1] are

$$\overline{\psi}_{m,j}=\frac{\psi_{m,j+\frac{1}{2}}+\psi_{m,j-\frac{1}{2}}}{2},$$
$$m=1:N, \qquad j=1:J. \tag{13}$$

The linear diamond method is equivalent to the classic implicit trapezoidal method for initial value problems [8]. In Eqs. (12) and (13) we have defined the cell-average angular flux

$$\overline{\psi}_{m,j}=\frac{1}{h_j}\int_{x_{j-\frac{1}{2}}}^{x_{j+\frac{1}{2}}}\psi_m(x)dx \tag{14}$$

and for the cell-average scalar flux, cf. Eq. (8), we approximate

$$\overline{\phi}_j=\sum_{n=1}^{N}\overline{\psi}_{n,j}\omega_n. \tag{15}$$

Furthermore, by using approximation (15) in the scattering source and substituting the auxiliary equation (13) into the collision removal term of Eq. (12), we obtain the result

$$\psi_{m,j\pm\frac{1}{2}}=\frac{\left[\frac{|\mu_m|}{h_j}-\frac{\sigma_{Tj}}{2}\left(1-|\theta_{m,j}|\right)\right]\psi_{m,j\mp\frac{1}{2}}+\frac{1}{2}\sigma_{Sj}\overline{\phi}_j+Q_j}{\left[\frac{|\mu_m|}{h_j}+\frac{\sigma_{Tj}}{2}\left(1+|\theta_{m,j}|\right)\right]},$$
$$m=1:N, \qquad j=1:J. \tag{16}$$

For an initial guess for $\overline{\phi}_j$, usually $\overline{\phi}_j=0$, $j=1:J$, Eq. (16) is used to sweep from left to right ($\mu_m>0$) and from right to left ($\mu_m<0$) to estimate the cell-edge angular fluxes. Then, we use Eqs. (13) and (15) to update the scattering source, before we proceed to the sweeps again, until a preassigned convergence criterion is satisfied. As we have described in section 1, this iterative scheme is referred to as the SI scheme; that can be very slow for scattering dominated slabs with many mean free

paths in extent.

In the next section, we describe an efficient procedure to improve the initial guess for the cell-average scalar flux $\bar{\phi}_j$, $j = 1{:}J$, in the scattering source term of Eq. (16).

3 THE COARSE-MESH DIFFUSION SYNTHETIC ACCELERATION

3.1 The neutron diffusion equation

To derive neutron diffusion equation in slab geometry, we use definition (8) in Eq. (1), then we integrate the resulting transport equation in all directions of flight. The procedure leads to the continuity equation

$$\frac{d}{dx} J(x) + \sigma_a(x)\phi(x) = 2Q(x), \tag{17}$$

where we have defined

$$J(x) = \text{total current} = \int_{-1}^{1} \mu\psi(x,\mu')d\mu' \tag{18a}$$

$$\sigma_a(x) = \text{absorption macroscopic cross section} = \sigma_T(x) - \sigma_S(x). \tag{18b}$$

Moreover, we consider the Fick's law approximation

$$J(x) = -D(x)\frac{d}{dx}\phi(x), \tag{19a}$$

where the diffusion coefficient is defined as

$$D(x) = \frac{1}{3\sigma_T(x)} \ . \tag{19b}$$

Fick's law (19a-b), the essence of neutron diffusion approximation, implies that particles migrate from regions of high concentration to regions of low concentration. Therefore, by substituting Eq. (19a) into Eq. (17), we obtain the steady-state, one speed, isotropically-scattering fixed source neutron diffusion equation in slab geometry

$$-\frac{d}{dx} D(x)\frac{d}{dx}\phi(x) + \sigma_a(x)\phi(x) = 2Q(x) \ . \tag{20}$$

The approximate boundary conditions to account for the prescribed boundary conditions given in Eq. (2)-(3) are described in the next section.

3.2 The S_2 boundary conditions

Let us consider the expansion of the angular flux in Legendre polynomials in the angular variable μ

$$\psi(x,\mu)=\sum_{\ell=1}^{L}\frac{(2\ell+1)}{2}\phi_\ell(x)P_\ell(\mu). \tag{21}$$

The P_1-approximation [1] considers L=1, $\phi_0(x)=\phi(x)$ [Eq. (8)], $\phi_1(x)=J(x)$ [Eq. (18a)] in Eq. (21) and the result is

$$\psi(x,\mu)=\frac{1}{2}\phi(x)+\frac{3}{2}\mu J(x). \tag{22}$$

For isotropic incoming angular fluxes at $x=0$ and $x=X$, Eq. (22) approximates Eqs. (2) and (3) by

$$f=\frac{1}{2}\phi(0)+\frac{3}{2}\mu J(0), \qquad \mu>0 \tag{23a}$$

and

$$g=\frac{1}{2}\phi(X)-\frac{3}{2}|\mu|J(X), \qquad \mu<0. \tag{23a}$$

Using Gauss-Legendre S_2 angular quadrature set, we have $\mu_1=\frac{\sqrt{3}}{3}$ and $\mu_2=-\frac{\sqrt{3}}{3}$; therefore we obtain

$$J(0)=\frac{2\sqrt{3}}{3}f-\frac{\sqrt{3}}{3}\phi(0) \tag{24a}$$

for the left-hand side boundary $(x=0)$ and

$$J(X)=-\frac{2\sqrt{3}}{3}g+\frac{\sqrt{3}}{3}\phi(X) \tag{24b}$$

for the right-hand side boundary $(x=X)$, where f and g are the prescribed isotropic incident angular flux at $x=0$ and $x=X$, respectively. If vacuum boundary conditions apply at $x=0$ and/or $x=X$, then we set $f=0$ and/or $g=0$ in Eqs. (24a-b).

3.3 The diffusion spectral nodal method

Let us consider a coarse-mesh spatial grid set up on a slab of thickness X, as shown in Figure 1. Now we write the continuity equation (17) and Fick's law (19a) for an arbitrary spatial discretization node Γ_j, to which we apply the operator

$$\frac{1}{h_j}\int_{x_{j-\frac{1}{2}}}^{x_{j+\frac{1}{2}}}(\cdot)dx \ .$$

The results are the discretized equations

$$\frac{J_{j+\frac{1}{2}} - J_{j-\frac{1}{2}}}{h_j} + \sigma_{aj}\bar{\phi}_j = 2Q_j \tag{25}$$

$$\bar{J}_j = -\frac{D_j}{h_j}\left(\phi_{j+\frac{1}{2}} - \phi_{j-\frac{1}{2}}\right) \tag{26}$$

Here we have defined the node-average quantities

$$\xi_j = \frac{1}{h_j}\int_{x_{j-\frac{1}{2}}}^{x_{j+\frac{1}{2}}} \xi(x)dx, \qquad \xi = J \quad or \quad \phi, \tag{27}$$

and the constant nodal parameters

σ_{aj} = macroscopic absorption cross section, $j = 1:J$;

D_j = diffusion coefficient, $j = 1:J$;

Q_j = interior isotropic fixed source, $j = 1:J$.

Now we seek for general analytic solution for $x \in \Gamma_j$ of the form

$$\phi(x) = a(\upsilon)e^{-\sigma_{aj}x/\upsilon} + \phi_j^P \tag{28}$$

$$J(x) = b(\upsilon)e^{-\sigma_{aj}x/\upsilon} + J_j^P. \tag{29}$$

By substituting Eqs. (28) and (29) into Eqs. (17) and (19a), we obtain

$$\sigma_{aj}e^{-\sigma_{aj}x/\upsilon}a(\upsilon) - \frac{\sigma_{aj}}{\upsilon}e^{-\sigma_{aj}x/\upsilon}b(\upsilon) = Q_j - \sigma_{aj}\phi_j^P \tag{30a}$$

$$-\frac{D_j\sigma_{aj}}{\upsilon}e^{-\sigma_{aj}x/\upsilon}a(\upsilon) + e^{-\sigma_{aj}x/\upsilon}b(\upsilon) = J_j^P. \tag{30b}$$

Here we obtain particular solutions given by $J_j^P = 0$ and $\phi_j^P = Q_j/\sigma_{aj}$, $j = 1:J$, and for non-trivial solutions we must have

$$\upsilon = \pm\sqrt{D_j\sigma_{aj}}. \tag{31}$$

Moreover, by choosing $a(\upsilon) = 1$, we obtain $b(\upsilon) = \sqrt{D_j\sigma_{aj}}$. Therefore, the within node general solutions (28) and (29) appear as

$$\phi(x) = e^{-x/L_j} + \frac{Q_j}{\sigma_{aj}} \tag{32a}$$

$$J(x) = \sqrt{D_j\sigma_{aj}}\,e^{-\sigma_{aj}x/L_j}, \quad x \in \Gamma_j, \tag{32b}$$

where we have defined the diffusion length

$$L_j = \sqrt{\frac{D_j}{\sigma_{aj}}}; \qquad j = 1:J. \tag{32c}$$

The diffusion spectral nodal method is a convergent numerical method whose solution satisfies the boundary conditions (24a-b), is continuous across the node edges and preserves the general solutions given by Eqs. (32a-c); therefore this numerical method is absolutely free from spatial truncation errors in the sense that the numerical solution coincides with the analytical solution of the diffusion problem on the discretization grid points, regardless of the node widths set up on the domain, but apart from computational finite arithmetic considerations. Therefore, we consider the auxiliary equations

$$\bar{\phi}_j = \frac{\gamma_j}{2}\left(\phi_{j+\frac{1}{2}} - \phi_{j-\frac{1}{2}}\right) + G(Q_j) \tag{33}$$

$$\bar{J}_j = \frac{\beta_j}{2}\left(J_{j+\frac{1}{2}} - J_{j-\frac{1}{2}}\right). \tag{34}$$

Using definition (27) and Eqs. (32a-c) in Eqs. (33) and (34), we obtain

$$G(Q_j) = \frac{(1-\gamma_j)Q_j}{\sigma_{aj}}, \tag{35a}$$

$$\gamma_j = \frac{2L_j}{h_j} tgh\left(\frac{h_j}{2L_j}\right), \tag{35b}$$

$$\beta_j = \gamma_j, \qquad j = 1:J. \tag{35c}$$

Now we substitute Eq. (33) into Eq. (25) and Eq. (34) into Eq. (26). We solve the resulting equations for $J_{j+\frac{1}{2}}$ and $J_{j-\frac{1}{2}}$, substitute j in the latter expression for $j+1$ and apply current continuity condition at $x_{j+\frac{1}{2}}$. The result is the three point equation

$$\left(-\frac{D_j}{\gamma_j h_j} + \frac{h_j \sigma_{aj}\gamma_j}{4}\right)\phi_{j-\frac{1}{2}} + \left(\frac{D_{j+1}}{\gamma_{j+1}h_{j+1}} + \frac{D_j}{\gamma_j h_j} + \frac{h_{j+1}\sigma_{aj+1}\gamma_{j+1}}{4} + \frac{h_j\sigma_{aj}\gamma_j}{4}\right)\phi_{j+\frac{1}{2}} +$$
$$+\left(-\frac{D_{j+1}}{\gamma_{j+1}h_{j+1}} + \frac{h_{j+1}\sigma_{aj+1}\gamma_{j+1}}{4}\right)\phi_{j+\frac{3}{2}} = \frac{\gamma_j h_j}{2}Q_j + \frac{\gamma_{j+1}h_{j+1}}{2}Q_{j+1} \tag{36}$$
$$j = 2:(J-1).$$

Furthermore, we set $j = 1$ in the expression that we obtained for $J_{j-\frac{1}{2}}$ and use the boundary condition at $x = 0$ (24a), that is

$$J_{\frac{1}{2}} = \frac{2\sqrt{3}}{3} f - \frac{\sqrt{3}}{3}\phi_{\frac{1}{2}}. \tag{37}$$

The result is the difference equation

$$\left(\frac{\sqrt{3}}{3}+\frac{D_1}{\gamma_1 h_1}+\frac{h_1\sigma_{a1}\gamma_1}{4}\right)\phi_{\frac{1}{2}}+\left(-\frac{D_1}{\gamma_1 h_1}+\frac{h_1\sigma_{a1}\gamma_1}{4}\right)\phi_{\frac{3}{2}}=\frac{2\sqrt{3}}{3}f+\frac{\gamma_1 h_1}{2}Q_1. \tag{38}$$

Similarly, we set $j=J$ in the expression that we obtained for $J_{j+\frac{1}{2}}$ and use the boundary condition at $x=X$ (24b), i.e.,

$$J_{J+\frac{1}{2}}=-\frac{2\sqrt{3}}{3}g+\frac{\sqrt{3}}{3}\phi_{J+\frac{1}{2}}. \tag{39}$$

The result is

$$\left(-\frac{D_J}{\gamma_J h_J}+\frac{h_J\sigma_{aJ}\gamma_J}{4}\right)\phi_{J-\frac{1}{2}}+\left(\frac{\sqrt{3}}{3}+\frac{D_J}{\gamma_J h_J}+\frac{h_J\sigma_{aJ}\gamma_J}{4}\right)\phi_{J+\frac{1}{2}}=\frac{2\sqrt{3}}{3}g+\frac{\gamma_J h_J}{2}Q_J. \tag{40}$$

Equations (38), (36) for $j=2:(J-1)$ and (40) form a symmetric tridiagonal system of $J+1$ algebraic equations in $J+1$ unknowns $\phi_{1/2}$, $\phi_{3/2}$, $\phi_{5/2}$, ..., $\phi_{J+1/2}$, which are the neutron scalar fluxes. We remark that these numerical values, as generated by the present spectral nodal method, are completely free from spatial truncation errors.

3.4 The nodal reconstruction scheme

Since the spectral nodal method generates numerical solutions for neutron diffusion problems in slab geometry that are free from spatial truncation errors, we can use the node-edge scalar fluxes and solve for the constants α_ℓ, $\ell=1:2$, in the expression for the general solution

$$\phi(x)=\sum_{\ell=1}^{2}\alpha_\ell e^{-\sigma_{aj}x/\upsilon_\ell}+\frac{Q_j}{\sigma_{aj}}, \qquad x\in\Gamma_j. \tag{41}$$

By determining the constants α_ℓ, $\ell=1:2$, we can reconstruct the within-node solution for each discretization node Γ_j, $j=1:J$. Moreover, we can determine the fine-mesh average scalar fluxes

$$\bar{\phi}_j=\frac{1}{h_j}\int_{x_{j-\frac{1}{2}}}^{x_{j+\frac{1}{2}}}\phi(x)dx=\frac{1}{h_j\sigma_{aj}}\sum_{\ell=1}^{2}\alpha_\ell\upsilon_\ell\left(e^{-\sigma_{aj}x_{j-1/2}/\upsilon_\ell}-e^{-\sigma_{aj}x_{j+1/2}/\upsilon_\ell}\right)+\frac{Q_j}{\sigma_{aj}} \tag{42}$$
$$x\in\Gamma_j, \qquad j=1:J,$$

that we use as initial guess in Eq. (16) for the source iteration scheme. Therefore, the present coarse-mesh DSA strategy uses improved initial guess for the isotropic scattering source as generated by the diffusion equation with S_2 boundary conditions as described in section 3.2.

4 NUMERICAL RESULTS

Let us consider a homogeneous slab of thickness 100 cm, with macroscopic total cross section σ_T =1.0 cm^{-1} and macroscopic scattering cross section σ_S =0.995 cm^{-1}. Unit incident neutron fluxes shine at x = 0 and x = 100 *cm*, i.e., $f = g = 1$ in Eqs. (10) and (11) with Gauss-Legendre S_{16} angular quadrature set. To solve this problem, we used the linear diamond method on a fine spatial grid composed of 2000 nodes and a convergence criterion requiring that the discrete maximum norm of the relative deviation between two consecutive estimates of the node-edge scalar flux does not exceed 10^{-6}. The number of iterations to convergence required by the non-accelerated SI scheme is 2158. Using the present coarse-mesh DSA scheme, the number of iterations reduced to 1349. That is, the number of iterations to convergence has been reduced of 37.5%. Our second numerical experiment consists of shortening the slab thickness of this model problem as $X_n = 100 - 10n$, n = 0 : 5. The results are displayed in Table 1.

Slab thickness (*cm*)	Non-accelerated SI scheme	Coarse-mesh DSA scheme	Relative efficiency
100	2158[a] (8.74seconds)[b]	1349[a] (5.57seconds)[b]	37.5%[c] (36.3%)[d]
90	2056[a] (8.37seconds)[b]	1265[a] (5.15seconds)[b]	38.5%[c] (38.5%)[d]
80	1949[a] (8.10seconds)[b]	1179[a] (4.65seconds)[b]	39.5%[c] (42.6%)[d]
70	1837[a] (7.14seconds)[b]	1091[a] (4.54seconds)[b]	40.6%[c] (36.4%)[d]
60	1713[a] (7.10seconds)[b]	1000[a] (4.00seconds)[b]	41.6%[c] (43.7%)[d]
50	1571[a] (6.58seconds)[b]	902[a] (3.80seconds)[b]	42.6%[c] (42.2%)[d]

a. number of iterations to convergence; b. CPU time to convergence; c. reduction of the number of iterations; d. reduction of CPU time

Table 1: Gauss-Legendre S_{16} homogeneous model problem.

In accordance with Table 1, as the slab shortens from 100 *cm* to 50 *cm*, the present

coarse-mesh DSA scheme becomes more and more efficient since the numbers of iterations to convergence to the same numerical results are reduced from 37.5% (100 *cm*) to 42.6% (50 *cm*). This good feature leads to shorter and shorter CPU execution time for each run, as it is also displayed in Table 1. The gain in CPU time for convergence of these numerical experiments turned out to be greater than 35% for all the cases we considered.

5 DISCUSSION

Based on the numerical results presented in the previous section, we list a number of general conclusions:

- the coarse-mesh DSA strategy is very efficient, as it accelerates the SI scheme by reducing the number of iterations to convergence in more than 35% for the numerical experiments considered in the previous section;
- the coarse-mesh DSA strategy, as described in this paper, shortened the CPU execution time in approximately 35% also. Although the running time is very short, even for the non accelerated schemes (less than 10 seconds), it is good to see that the present coarse-mesh DSA converged the solution to the same results 35% faster. We believe that the present strategy will show its potential significant efficiency in multidimensional S_N calculations;
- for acceleration efficiency, it is important to use accurate boundary conditions in the diffusion equation to account for the prescribed incident flux S_N boundary conditions.

As future work, we intend to apply the present coarse-mesh DSA strategy to accelerate linearly anisotropic scattering and multigroup problems to account for the neutron energy change in scattering events.

ACKNOWLEDGEMENTS

This research work is part of the project of the National Institute of Science and Technology on Innovative Nuclear Reactors (INCT/CNPq – FAPERJ, Brazil). The first author (FPS) acknowledges the financial support given by CAPES (Brazil) and the second author (VSX) is sponsored by FAPERJ (RJ, Brazil).

REFERENCES

[1]E. E. Lewis, W. F. Miller Jr., Computational Methods of Neutron Transport, *American Nuclear Society, La Grange Park, Illinois*, 1993.

[2]M. L. Adams, E. W. Larsen, Fast Iterative Methods for Discrete-Ordinates Particle transport Calculations, *Progress in Nuclear Energy*, Vol. 40, N° 1, pp 3-159, 2002.

[3]H. J. Koop, Synthetic Method Solution of the Transport Equation, *Nuclear Science and Engineering*, Vol. 17, pp 65, 1963.

[4]J. J. Duderstadt, W. R. Martin, Transport Theory, *John Wiley & Sons*, New York,

1979.
[5]W. H. Reed, The Effectiveness of Acceleration Techniques for Iterative Methods in Transport Theory, *Nuclear Science and Engineering*, Vol. 45, pp 245, 1971.
[6]R. E. Alcouffe, A Stable Diffusion Synthetic Acceleration Method for Neutron Transport Iterations, *Transactions American Nuclear Society*, Vol. 27, pp 346, 1977.
[7]R. C. Barros, On the Equivalence of Discontinuous Finite Element Methods and Discrete ordinates Methods for the Angular Discretization of the Linearized Boltzmann Equation in Slab Geometry, *Annals of Nuclear Energy*, Vol. 24, pp 1013, 1997.
[8]R. L. Burden, J. D. Faires, Numerical Analysis, 8th Ed., New York, 1993.